JOURNAL OF MATERIALS SCIENCE 21 (1986) 3717–3723

A humidity sensor using burned zircon with phosphoric acid: effect of strongly acidic protons on humidity sensitivity

YOSHIHIKO SADAOKA, YOSHIRO SAKAI
Department of Industrial Chemistry, Faculty of Engineering, Ehime University, Matsuyama 790, Japan

Impedance and water sorption measurements have been made of burned zircon with phosphoric acid. In a humid atmosphere, the resistance which is approximated by the impedance is inversely proportional to the concentration of the strongly acidic PO–H group which results in an increase in the sorbed water. The addition of the strongly acidic PO–H formed on the particle surfaces leads to decreases in the resistance and its activation energy. For the element burned at 350° C in which the $H_3PO_4/ZrSiO_4$ mole ratio is 0.2 or more, the resistance is $10^6\,\Omega$ or below in a dry atmosphere and decreases with an increase in humidity. The humidity dependence of the resistance can be controlled not only by the form of the porous insulating ceramic but also by the addition of the strongly acidic protons. The response times of the resistance for the surface-type element to the humidity changes are 3 min or below for both adsorption and desorption processes.

1. Introduction

Many types of porous oxide [1–6] have been proposed for humidity sensors. For humidity sensors using porous oxides, the admittance is usually enhanced by the adsorption of water and/or capillary condensation of water. Upon exposure to the atmosphere, strongly bound water molecules quickly occupy the available sites of porous oxides. Once the first layer has been formed, subsequent layers of water molecules are physically adsorbed. When water molecules are present, but surface coverage is not complete, H_3O^+ diffusion and H^+ hopping and/or transfer occur on the surface. When water molecules are abundant, the physisorbed water dissociates due to the high electrostatic field in the chemisorbed layer:

$$2H_2O \rightleftharpoons H_3O^+ + OH^-$$

Charge transport occurs when the hydronium ion releases a proton to a neighbouring water molecule (the Grotthuss chain reaction) [7]. Porous oxides are adequate for conventional humidity sensing devices. However, the usual metal oxide has some disadvantages; the impedance is $10^8\,\Omega$ cm or more in the low-humidity region and so it is difficult to detect humidity variation by using a conventional impedance meter. In order to overcome this disadvantage, the addition of a mobile ion such as proton and alkali ion into the porous oxide was considered. Previously, it has been reported that zircon sintered with phosphoric acid as a binder at 1000° C is desirable in a humidity sensor that will have better sensitivity and stability [8], while the impedance is $10^8\,\Omega$ cm or more in the low-humidity region. It is confirmed that the addition of a dissociative proton formed on the particle surface results in a decrease in the impedance. This paper presents the results of a study investigating the effects of the strongly acidic PO–H groups, formed on the particle surface, on the hygroscopic and electrical properties of burned zircon film with phosphoric acid.

2. Experimental procedure

Fine-particle zircon (average particle diameter, 1 μm) and phosphoric acid were used. The raw materials were weighed in the prescribed mole ratio and mixed using water as a mixing medium. The slurry coated on the substrate (α-Al_2O_3) with one pair of gold electrodes was dried at 60° C and burned at various temperatures. The thickness of the film is about 0.01 cm (surface-type element). Sandwich-type elements were prepared as follows. The mixed material was pressed into a disc, dried at 350° C and finally sintered at various temperatures. The ceramic body obtained was then shaped to 0.05 cm × 1 cm × 1 cm. Next, RuO_2 electrodes, 0.4 cm × 0.4 cm, were applied to opposite faces of the ceramic body by printing and heating at 800° C for 20 min.

α-zirconium phosphate and amorphous zirconium phosphate were prepared by the method described by Andersen *et al.* [9].

The crystalline phases were identified at room temperature by standard X-ray diffraction techniques. The microstructure was examined by scanning electron microscopy. The pore size distribution was examined by means of mercury penetration porosimetry. The specific surface area was determined by the BET method using N_2 as a sorbate. The amount of sorbed water was determined by gravimetric analysis. The concentration of strongly acidic protons was

0022–2461/86 $03.00 + .12

TABLE I Characteristic values for burned samples and zircon powder

Sample	$H_3PO_4/ZrSiO_4$ (mole ratio)*	Burning temperature (° C)	True specific gravity ($g\,cm^{-3}$)	Pore volume ($7\,\mu m > r > 3.2\,nm$)† ($cm^3\,g^{-1}$)	Surface area, S_{N_2} ($m^2\,g^{-1}$)	C_{HS} ($mol\,g^{-1}$) × 10^4
ZP-1- 350	0.5	350	4.3	0.105	1.9	1.85
ZP-2- 350	0.2	350	4.4	1.182	2.8	1.35
ZP-3- 350	0.1	350	4.6	0.207	3.6	0.30
ZP-4- 350	0.05	350	4.7	0.233	6.0	0.15
ZP-5- 350	0.02	350	4.7	0.278	8.6	0.15
ZP-2- 500	0.2	500	4.5	0.197	2.5	1.70
ZP-3- 500	0.1	500	4.5	0.240	3.0	0.83
ZP-4- 500	0.05	500	4.7	0.282	4.8	0.45
ZP-2- 700	0.2	700	4.3	0.185	3.3	0.92
ZP-3- 700	0.1	700	4.7	0.182	3.7	0.46
ZP-4- 700	0.05	700	4.3	0.221	5.7	0.25
ZP-1- 600‡	0.5	600, 800	4.1	0.051	2.76	1.1
ZP-1- 800‡	0.5	800, 800	4.2	0.054	2.19	0.5
ZP-1-1000‡	0.5	1000, 800	4.0	0.051	1.92	0.03
$ZrSiO_4$	–	–	4.56	–	9.3	–

*Components of raw materials.
†r = pore radius.
‡Compressed discs burned at a given temperature, followed by at 800° C for 20 min.

examined by the method of pH titration with 0.1 N NaOH solution.

Humidity–impedance characteristics were measured with impedance meters (Yokogawa Hewlett Packard 4276A and 4277A). Relative humidities (% r.h.), ranging from 0 to 90, were achieved by mixing dry and moist air in controlled proportions.

3. Results

3.1. Form of sample

For the samples burned at 800° C and below, all the observed X-ray diffraction peaks were assigned to zircon ($20° < 2\theta < 60°$, Cu$K\alpha$), i.e. no new crystalline phase formation could be detected. The true specific gravity, the pore volume determined by mercury porosimetry and the surface area determined by the BET method using N_2 as a sorbate are summarized in Table I. While the true specific gravity is poorly dependent on the $H_3PO_4/ZrSiO_4$ mole ratio in the raw materials and burning temperature, the pore volume and the surface area have a tendency to increase with decreasing $H_3PO_4/ZrSiO_4$ mole ratio and, in particular, the surface area of the burned sample is less than that of the powder of virgin zircon. Furthermore, the average pore radius for burned samples is estimated to be 100 to 170 nm.

3.2. pH titration curves

0.1 g of sample was equilibrated with 50 ml of a solution containing NaCl. The solution was then acidified. In titrating the solution with 0.1 N of NaOH solution, two neutralization points were confirmed at pH 5.0 and pH 8.5. From the titration curves, the concentration of strongly acidic protons can be estimated by the point at pH 5 and that of weakly acidic proton by the point at pH 8.5. The concentration of both types of acidic proton decreases with increases in the burning temperature and with decreasing $H_3PO_4/ZrSiO_4$ mole ratio in the raw material. The concentration of the strongly acidic protons, C_{HS}, is summarized in Table I.

3.3. Water sorption isotherms and thermal gravimetric analysis

In Fig. 1, the humidity dependence of the amount of sorbed water is shown. The water adsorption isotherms measured immediately after preparing the burned samples are shown by broken curves. The solid curves indicate the water sorption isotherms of samples permitted to stand at 90° C for 16 h in contact with moist air. An increase in weight is achieved by this exposure to moist air. Similar tendencies were confirmed in all samples. It seems that this increase in weight is caused by the resorption of water and the formation of PO–H based on the hydrolysis of

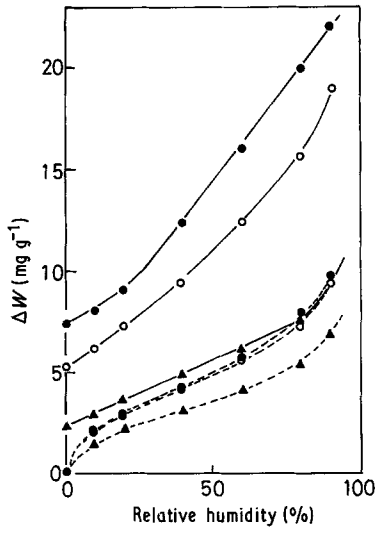

Figure 1 Water sorption isotherms at 30° C for samples burned at 350° C: (●) ZP-2, (○) ZP-3, (▲) ZP-4. Broken lines: burned immediately before measuring isotherm. Solid lines: exposed to moist atmosphere at 90° C immediately before measuring isotherm.

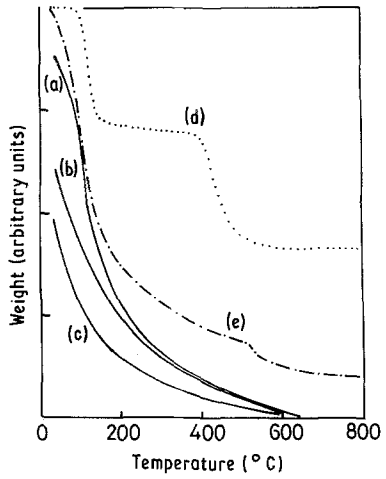

Figure 2 TG curves for samples (a) ZP-2-350, (b) ZP-3-350, (c) ZP-4-350, (d) α-$Zr(HPO_4)_2 \cdot H_2O$, (e) amorphous $Zr(H_2PO_4)_2 \cdot xH_2O$. The samples of ZP were exposed to a moist atmosphere at 90° C immediately before measuring. Heating rate: 8° C min^{-1}, flow rate of helium gas: 40 ml min^{-1}. Weight increased upwards on the vertical scale.

P–O–P groups. It is expected that the contribution of these processes can be distinguished by the method of thermal gravimetry (TG). In Fig. 2, the TG curves are shown. For reference, the results for α-zirconium phosphate (α-$Zr(HPO_4)_2 \cdot H_2O$) [9] and amorphous zirconium phosphate ($ZrO(H_2PO_4)_2 \cdot H_2O$) [9] are shown. While two plateaux are confirmed in the TG curve for α-zirconium phosphate, no apparent plateaux can be detected in those for the burned samples and these results are similar in pattern to that for amorphous zirconium phosphate. The contributions of these processes cannot therefore be distinguished.

The increase in weight of the samples permitted to stand at 90° C for 16 h in contact with moist air is affected by the $H_3PO_4/ZrSiO_4$ mole ratio and the burning temperature, and is shown in Fig. 3 as a function of the concentration of the strongly acidic PO–H. In this case, it is assumed that the increase in weight is proportional to the surface area. Line (b) in

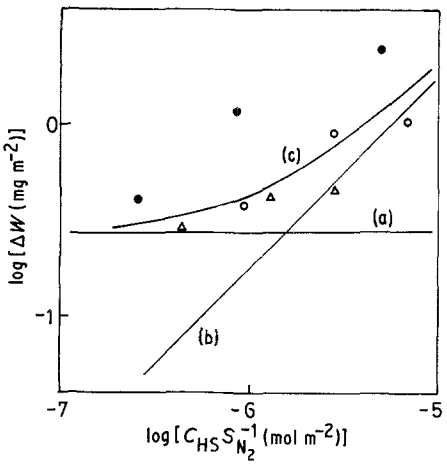

Figure 3 Relationship between ΔW and surface density of strongly acidic protons at 0 % r.h. for samples exposed to a moist atmosphere at 90° C. Burning temperature: (●) 350, (○) 500, (△) 700° C. (a) Weight of sorbed water to form a monolayer of water; (b) weight corresponding to the reaction P–O–P → 2P–O–H; (c) sum of (a) and (b).

Fig. 3 indicates the expected increment in weight accompanying the reaction of PO–H regeneration (the hydrolysis of P–O–P groups):

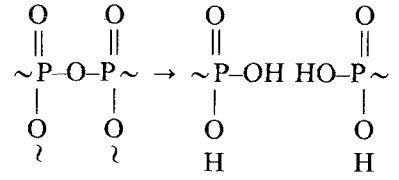

Line (a) in Fig. 3 indicates the increment in weight caused by the formation of the first layer of physisorbed water. The sum of both increments in weight is expressed by Curve (c). While the results of the samples burned at 500 and 700° C correspond to Curve (c), a distinct deviation from this curve is confirmed on the samples burned at 350° C. The increase in weight of the sample burned at 350° C is considerably larger than that accompanying the following reaction:

$$P_2O_5 + 3H_2O \rightarrow 2H_3PO_4$$

This suggests that sorbed water exists in the surface layer even in a dry atmosphere. The PO_4 groups may exist on zircon surfaces in the form of self-condensed phosphoric acid and phosphuretted zircon, and the latter form increases with the burning temperature. In addition, the latter form may be more stable than the former which is easily hydrolysed and dissolved in water. While it is not possible to determine the structure of the phosphoric compounds formed on the surfaces, the increase in impedance with the washing of the sample by water is inhibited by an increase in the burning temperature. This means that most of the phosphoric compound formed in the sample burned at 350° C exists as self-condensed phosphoric acid, and the amount of this compound decreases with the burning temperature.

3.4. Humidity dependence of impedance

The complex impedance has been employed to analyse the impedance measurements since it seems that the impedance consists of resistive and capacitive components. Complex impedance plots are shown in Fig. 4. The high-frequency results are represented by nearly perfect circular arcs, all of which pass through the origin. In addition, at low frequencies a second arc or spur observed in the high-humidity region may arise from electrode polarization. The resistance components, R_p, are easily estimated from the intercepts of circular arcs and/or spurs with the real axes in the low-frequency region. In the region below $10^7\ \Omega$ of impedance, it is confirmed that the resistance can be approximated to the impedance at 1 kHz. In addition, it is confirmed that the capacitive component inserted in parallel with the resistance component is scarcely dependent on the humidity as listed in Table II.

In Fig. 5 the humidity dependence of resistance measured immediately after preparing the sample burned at 350° C is shown. For all samples, the resistance decreases with increasing humidity and the $H_3PO_3/ZrSiO_4$ mole ratio in the raw material.

The results for samples permitted to stand at 90° C

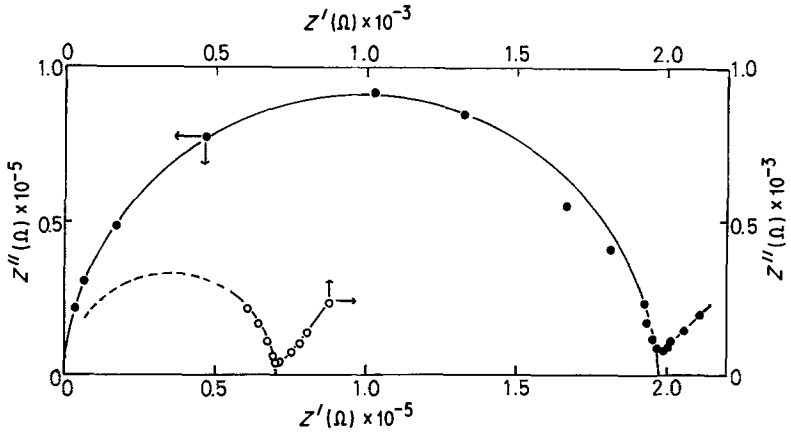

Figure 4 Complex impedance curves for ZP-3-400: (●) 30 % r.h., (○) 70 % r.h.

for 16 h in contact with moist air are shown in Fig. 6. Except for Sample ZP-5, the resistance decreases by exposure to moist air at each humidity. The humidity–resistance characteristics for the sample permitted to stand for 16 h in contact with moist air were reproducible with the humidity change. Fig. 7 shows the humidity dependence of resistance for samples permitted to stand for 16 h in contact with moist air after preparing samples burned at 500 and 700° C. It is confirmed that the resistance at each humidity decreases with increasing $H_3PO_4/ZrSiO_4$ mole ratio.

The response of the impedance to alteration in the humidity was examined. For all samples, a constant value of the impedance is observed within 3 min, after which the humidity is changed. This response time is considerably faster than that of the sandwich-type elements in which the interelectrode distance is 0.05 cm.

Since the conductance is strongly enhanced by the sorption of water and the concentration of strongly acidic protons, it seems that the main carriers are dissociative protons and hydrated protons (H_3O^+) which migrate in the surface layer of particles. In addition, the carrier may be produced by the dissociation of sorbed water and the strongly acidic PO–H groups. The extent of dissociation can be approximated from the equilibrium constant, K, for the dissociation reaction

$$K_{H_2O} = \frac{[H^+]\,[OH^-]}{[H_2O]} = \exp\left(\frac{\Delta S_1}{k}\right)\exp\left(\frac{-\Delta H_1}{kT}\right) \quad (1)$$

for H_2O and

$$K_{PO-H} = \frac{[H^+]\,[PO^-]}{[PO-H]} = \exp\left(\frac{\Delta S_2}{k}\right)\exp\left(\frac{-\Delta H_2}{kT}\right) \quad (2)$$

for PO–H groups, respectively. By making use of the requirement for electrical neutrality, the carrier concentration n can be expressed as $n \propto [H_2O]^{1/2}$ and $n \propto [PO-H]^{1/2}$. Here ΔS and ΔH are the carrier formation entropy and enthalpy, respectively, k is the Boltzmann constant and T is the absolute temperature. If strongly acidic protons from the phosphorus atom exist in a perfectly dissociated form, the carrier concentration is equal to the concentration of the strongly acidic protons, i.e.

$$n = [PO-H] \quad (3)$$

On the other hand, proton transport, in general, is governed by the jump probability of protons into the trapping and/or hopping sites. The jump frequency, W_j, depends upon the potential barrier and is expressed as

$$W_j = \nu_0 \exp\left(\frac{\Delta S}{k}\right)\exp\left(\frac{-\Delta H}{kT}\right) \quad (4)$$

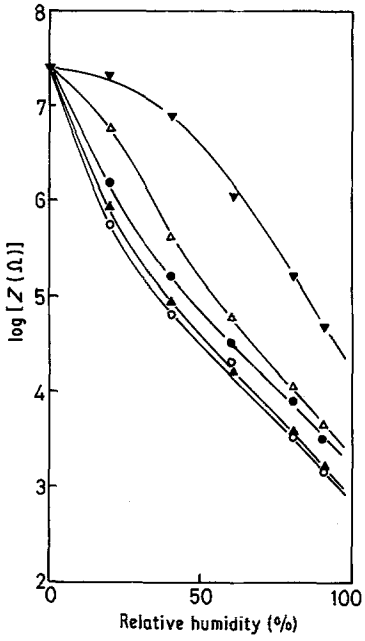

Figure 5 Humidity dependence of impedance at 30° C for virgin samples burned at 350° C immediately before measuring impedance: (●) ZP-1, (○) ZP-2, (▲) ZP-3, (△) ZP-4, (▼) ZP-5.

TABLE II Capacitive component (in pF) inserted in parallel with resistive component

Sample	Humidity (% r.h.)				
	10	30	50	70	90
ZP-3-400	8.29	8.53	8.65	–	–
ZP-4-400	–	9.59	8.06	9.91	8.38
ZP-5-400	–	7.80	9.47	7.23	7.65

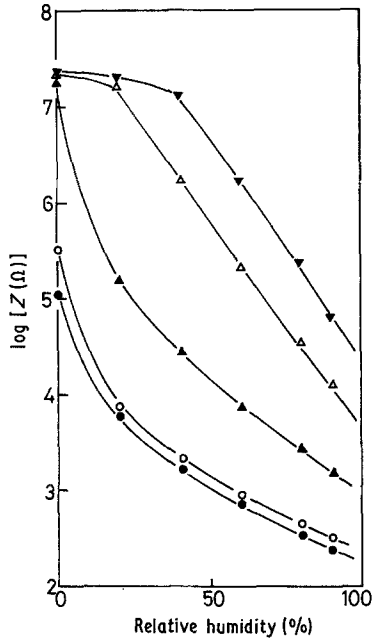

Figure 6 Humidity dependence of impedance at 30° C for samples burned at 350° C. The symbols are the same as in Fig. 5. All samples were exposed to a moist atmosphere at 90° C immediately before measuring impedance.

where ν_0 is the vibrational frequency for a carrier, ΔS is the entropy of migration and ΔH is the enthalpy of migration. For this system, the adsorbed water should act as a trapping and/or hopping site for the mobile protons. Finally, the conductivity, σ, is given by

$$\sigma = na^2e^2W_j/kT \quad (5)$$

where a is the jump distance and e is the charge element.

It is well known that $ZrSiO_4$ is an insulator, so the conductive path may be formed on zircon particles surrounded by phosphoric compounds and the sorbed water existing on the particle surfaces. For such inhomogeneous samples, the conductive path is complex and affected by the form of both particles and pores. Previously, the effects of the form of pore (particle size, pore diameter) and the surface area on the resistance of porous ceramics (insulators) have been studied [4]. According to these results, the resistance of porous ceramics in a humid atmosphere is inversely proportional to the surface area. As indicated in Table I, the surface area is affected by the burning conditions and the $H_3PO_4/ZrSiO_4$ mole ratio. To eliminate the effect of the surface area, the impedances of samples with 1 $m^2 g^{-1}$ surface area were estimated by the extrapolation method, by assuming that the resistance is inversely proportional to the surface area. The relationships between these extrapolated values of resistance and the surface concentration of the strongly acidic PO–H are shown in Figs 8 and 9. For the sample in which the concentration of strongly acidic PO–H is 5×10^{-6} mol m^{-2} or more, it is confirmed that the resistance is inversely proportional to the concentration of the PO–H group in a humid atmosphere, and the slope of the line increases gradually with decrease in humidity. In the region of lower concentrations of the PO–H group, a deviation from the linear relationship can be confirmed in Fig. 8. It seems that the solubility product of PO–H groups is poorly dependent on the concentration of PO–H groups, so that this deviation is interpretable in terms of an alteration of the proton transport mechanism [7] which may be affected by the coverage of physisorbed water as previously mentioned.

In Fig. 10 the relationship between the corrected impedance and the physisorbed water per 1 m^2 of surface area is shown. For both samples, similar relationships between both characteristics were confirmed,

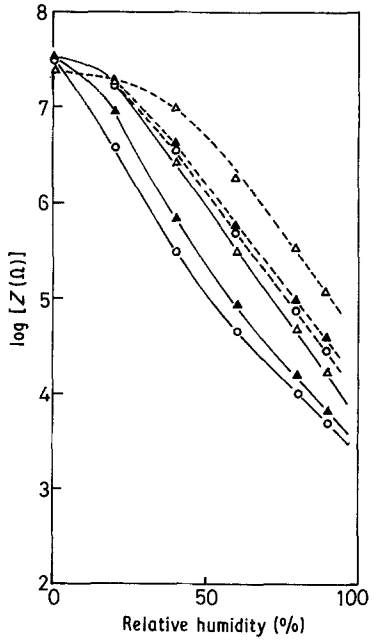

Figure 7 Humidity dependence of impedance at 30° C for samples exposed to a moist atmosphere at 90° C immediately before measuring impedance: (○) ZP-2, (▲) ZP-3, (△) ZP-4. Solid curves: burned at 500° C. Broken curves: burned at 700° C.

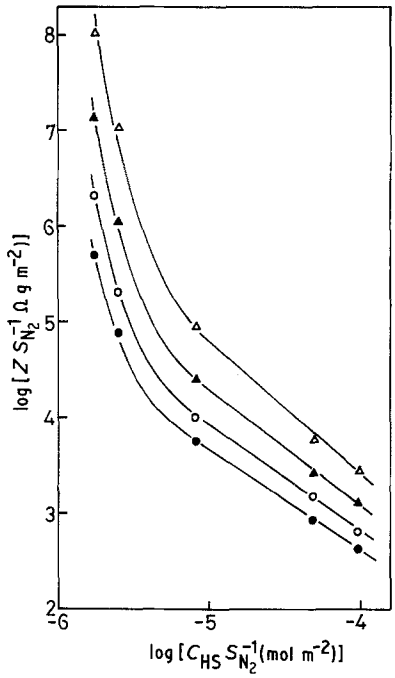

Figure 8 Relationship between $ZS_{N_2}^{-1}$ and $C_{HS}S_{N_2}^{-1}$ at 30° C for samples burned at 350° C and exposed to a moist atmosphere at 90° C immediately before measuring impedance. (●) 90 % r.h., (○) 80 % r.h., (▲) 60 % r.h., (△) 40 % r.h.

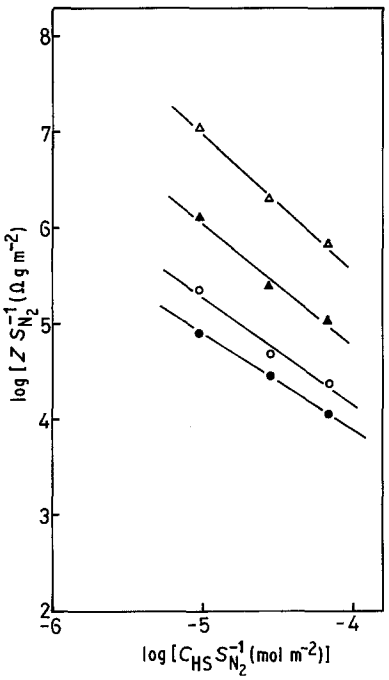

Figure 9 Relationship between $ZS_{N_2}^{-1}$ and $C_{HS}S_{N_2}^{-1}$ at 30° C for samples burned at 500° C and exposed to a moist atmosphere at 90° C immediately before measuring impedance. The symbols are the same as in Fig. 8.

and the impedance of ZP-4-350 is larger than that of ZP-3-350 by a factor of 4.0 and, in addition, the concentration of the strongly acidic PO–H groups in ZP-3-350 is larger than that in ZP-4-350 by a factor of 3.3. A fair agreement between both values indicates that the deviation is interpretable in terms of a difference in the coverage of physisorbed water. In this case, the amount of physisorbed water is approximated to the difference between the total weight at each humidity and the weight at 0% RH. If the conductive path consists only of the continuous water layer and the number of conductive paths (filaments) decreases with decrease in humidity and in addition, the concentration of carrier is limited by the solubility product of the sample, it is expected that the $ZS_{N_2}^{-1}$

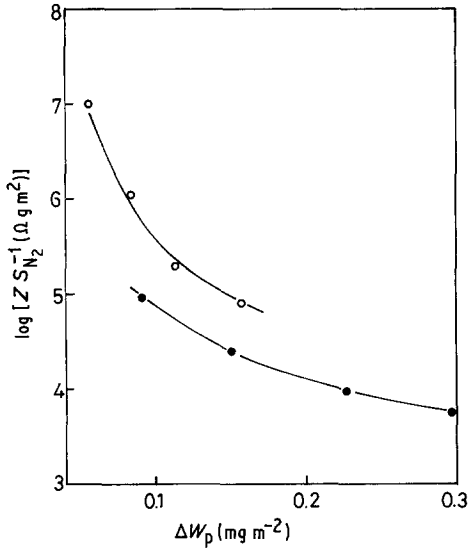

Figure 10 Relationship between $ZS_{N_2}^{-1}$ and ΔW_p at 30° C. (●) ZP3-350, (○) ZP4-350.

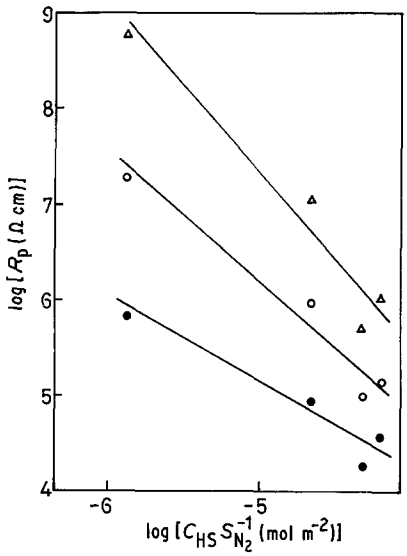

Figure 11 Relationship between R_p and $C_{HS}S_{N_2}^{-1}$ at 30° C for sandwich-type elements for which the $H_3PO_4/ZrSiO_4$ mole ratio is 0.5. (●) 90% r.h., (○) 60% r.h., (△) 30% r.h. The product $C_{HS}S_{N_2}^{-1}$ is altered by change of burning temperature from 350 to 1000° C.

value is inversely proportional to the physisorbed water and the activation energy of resistance is scarcely dependent on the humidity and the water content.

While the resistance decreases with increase in physisorbed water, the absolute value of the slope in Fig. 10 is higher than unity and increases with a decrease in physisorbed water, and the activation energy of resistance increases with a decrease in humidity as shown in Table III. These variations of slope in Fig. 10 and the activation energy with humidity can be explained qualitatively in terms of the variation of movability of charge carrier with physisorbed water, i.e. a change from the Grotthuss chain reaction to H_3O^+ diffusion and/or H^+ transfer with decreasing humidity. In addition, the increase in the slope of the line with decreasing humidity appearing in Figs 8 and 9 may be explained by an alteration of the charge transport mechanism which may be governed by the coverage of physisorbed water. With regard to this point, it has been reported [10] that the activation energy of the resistance of porous insulators without any strongly acidic protons decreases with an increase in the coverage of physisorbed water in the range in which the coverage is less than 2, while the activation energy is constant and the resistance is inversely proportional to the amount of water which is estimated by subtracting the amount needed to form a double physisorbed layer from the amount of total physisorbed water in the range in which the coverage of physisorbed water is larger than 2. These results indicate that the Grotthuss chain reaction is predominantly occurring in the physisorbed layer, especially in the range in which the coverage is larger than 2. As shown in Figs 3 and 6, the impedance of ZP-1-350 and ZP-2-350 is $10^{-6}\Omega$ or below and a considerable amount of sorbed water exists even in a dry atmosphere. In this way, the addition of the strongly acidic protons formed on the particle surfaces is preferred as a method of improvement of the humidity–impedance characteristic of ceramic humidity sensors.

TABLE III Activation energy (in eV) of resistance

% RH	ZP-3-400*	ZP-4-400*	ZP-5-400*	ZP-1-600†	ZP-1-800†	ZP-1-1000†
30	0.27	0.52	0.37	0.46	0.50	0.55
50	0.32	0.51	0.53	–	–	–
60	–	–	–	0.40	0.41	0.45
70	0.21	0.36	0.35	–	–	–
90	0.18	0.21	0.20	0.30	0.30	0.31

*Surface-type element.
†Sandwich-type element.

On the other hand, by comparison of the individual results of surface-type elements, a distinction in resistance between samples burned at different temperatures is noted, in spite of the fact that the concentration of the strongly acidic PO–H groups is the same. It seems that this distinction is caused by differences in sample thickness. To confirm this hypothesis, a sandwich-type element with controlled electrode area and interelectrode distance was prepared by using a sample in which the $H_3PO_4/ZrSiO_4$ mole ratio was 0.5. In this case, the concentration of the strongly acidic PO–H group was altered by variation of the burning temperature in the region from 350 to 1000° C. The relationship between the resistivity and the concentration of PO–H groups is shown in Fig. 11. It is confirmed that the resistance is inversely proportional to the concentration of PO–H groups at 90 % RH and the slope of the line increases gradually with a decrease in humidity. From these confirmed results, it is concluded that the humidity–resistance characteristic can be controlled not only by the form of the porous ceramic but also by the concentration of strongly acidic protons.

References

1. T. SEIYAMA, N. YAMAZOE and H. ARAI, *Sensors and Actuators* **4** (1983) 85.
2. T. NITTA, *Ind. Eng. Chem. Prod. Res. Dev.* **20** (1981) 669.
3. F. UCHIKAWA and K. SHIMAMOTO, *Amer. Ceram. Soc. Bull.* **64** (1985) 1137.
4. Y. SADAOKA and Y. SAKAI, *Denki Kagaku* **51** (1983) 879.
5. *Idem*, in Proceedings of International Meeting on Chemical Sensors, Fukuoka, September 1983, edited by T. Seiyama, K. Fueki, J. Shiokawa and S. Suzuki (Kodansha-Elsevier, Tokyo, 1983) p. 416.
6. *Idem, J. Mater. Sci.* **20** (1985) 3027.
7. J. H. ANDERSON and G. A. PARKS, *J. Phys. Chem.* **72** (1964) 3668.
8. Y. SADAOKA and Y. SAKAI, *Denki Kagaku* **51** (1983) 285.
9. E. K. ANDERSEN, I. G. K. ANDERSEN, C. K. MØLLER, K. E. SIMONSEN and E. SKOU, *Solid State Ionics* **7** (1982) 301.
10. Y. SADAOKA and Y. SAKAI, *Hyomen Kagaku* **5** (1984) 220.

Received 19 November 1985
and accepted 10 January 1986